

# Deformation and seismicity of Taiwan

Claudio Vita-Finzi\*

Department of Geological Sciences, University College, Gower Street, London WC1E 6BT, United Kingdom

Communicated by Luna B. Leopold, University of California, Berkeley, CA, August 7, 2000 (received for review April 10, 2000)

**<sup>14</sup>C-dated Holocene coastal uplift, conventional and satellite geodetic measurements, and coseismic and aseismic fault slip reveal the pattern of distributed deformation at Taiwan resulting from convergence between the Philippine Sea plate and Eurasia; as in other subduction orogenic settings, the locus of strain release and accumulation is strongly influenced by changes in fault geometry across strike. Uplift evidence from the islands of Lutaο and Lanhsu is consistent with progressive oblique collision between the Luzon arc and the Chinese continental margin. In the Coastal Range, geodetic and seismic records show that shortening is taken up serially by discontinuous slip on imbricate faults. The geodetic data point to net extension across the Central Range, but deformed Holocene shorelines in the Hengchun Peninsula at its southern extremity suggest that the extension is a superficial effect partly caused by blind reverse faulting. The fastest shortening rates indicated by geodesy are recorded on the Longitudinal Valley fault and across the Chukou fault within the fold-and-thrust belt. In the former, the strain is dissipated mainly as aseismic reverse and strike-slip displacement. In contrast, the fold-and-thrust belt has witnessed five earthquakes with magnitudes of 6.5 or above in the 20th century, including the 1999.9.21 Chi-Chi earthquake (magnitude  $\approx 7.6$ ) on a branch of the Chukou fault. The neotectonic and geodetic data for Taiwan as a whole suggest that the fold-and-thrust belt will continue to host the majority of great earthquakes on the island.**

neotectonics | geodesy | radiocarbon | subduction

Taiwan lies at the boundary between the Eurasian plate and the Philippine Sea plate (Fig. 1). To the northeast, the Philippine Sea plate is being subducted beneath Eurasia along the Ryukyu trench; to the south, subduction is in the opposite sense, and the Philippine Sea plate overrides Eurasia at the Manila trench. Between these two trench systems, the Philippine Sea plate collides obliquely with Eurasia at  $\approx 70\text{--}80$  mm/yr (1, 2), and the suture between them is propagating southwards at  $\approx 90$  mm/yr (3).

The major structural units of Taiwan are, from west to east, the Coastal Plain, the fold-and-thrust belt, the Central Range, the Longitudinal Valley, and the Coastal Range (Fig. 2). It is generally accepted that the fold-and-thrust belt and the Central Range (and their offshore extension the Hengchun Ridge) form part of the accretionary wedge and that the islands of Lanhsu and Lutaο form part of the Luzon volcanic arc on the edge of the Philippine Sea plate (4). The Coastal Range also falls within the Luzon arc in some schemes, whereas in others it is the northern extension of the Huatung Ridge, whose uplift results from motion on east-verging thrusts along the arc side of the accretionary wedge (5).

The rate of crustal shortening indicated by summing the seismic moment tensors of large earthquakes falls well short of the long-term plate convergence rate (6). As elsewhere, the deficit may be ascribed to aseismic deformation or to incompatibility between the periods being compared. The record of Holocene emergence on the eastern coast of central Taiwan (7) supports both arguments, because it suggests that shortening in the Coastal Range takes place seismically on reverse imbricate faults, which are activated serially and are therefore likely to be omitted from short instrumental catalogs, and aseismically on

strike-slip faults within the Coastal Range as well as along the Longitudinal Valley at its rear (8).

The present article seeks to discover whether the excess strain is preferentially stored and released in specific structural units on the island, because any such finding would be of obvious benefit to seismic zoning. To this end, the analysis is extended eastwards to include part of the Luzon arc off Taiwan, southwards to include the uplift record of the Central Range in the Tengshun Peninsula, and westwards to include recent seismicity in the fold-and-thrust belt. The data in question are consequently at three time scales, geological, geodetic, and coseismic; the hope is that they will prove to be complementary. The study draws on the work of numerous geodesists, geologists, and seismologists as well as the results of fieldwork and <sup>14</sup>C dating of coastal sequences by the writer.

**Neotectonics.** Paleoshoreline data for the eastern Coastal Range indicated Holocene uplift rates of between  $\approx 3$  and 5 mm/yr (7), an order of magnitude slower than that indicated by plate kinematics, and pointed to intermittent distributed deformation within the Coastal Range. Analysis of Holocene vertical movements on the islands of Lutaο and Lanhsu has now been undertaken to establish how far the Luzon arc is deforming as a unit and on the Hengchun Peninsula at the southern extremity of Taiwan to evaluate distortion of the Central Range. Field reports on the effects of the 1999 Chi-Chi earthquake provided an opportunity to assess the pattern of coseismic surface movement at the western margin of the fold-and-thrust belt. Paleoshoreline deposits were dated by <sup>14</sup>C assay of included coral and mollusk assemblages. The results amount to maximum ages, because the material is generally not in life position, but, in compensation, the ages bear on well defined waterlines. For consistency, all of the dates have been calibrated to calendar ages and corrected for the glaciohydroisostatic component of sea-level change as in the previous study (7).

A number of <sup>14</sup>C and U series ages on coral have already been reported from Lanhsu and Lutaο (9). After eustatic correction (but without correction for the depth favored by the coral), they indicated an uplift rate of  $\approx 3.8$  mm/yr for the two islands. The same sea-level correction curves had previously yielded uplift rates of  $5.0 \pm 0.2$  mm/yr for the eastern coastal area and  $5.3 \pm 0.2$  mm/yr for southern Taiwan (10), in good agreement with the average of 5 mm/yr obtained (7) for the southern segment of the Coastal Range.

The data for the two islands are given in Table 1; they include two of the published ages for Lutaο (9) calibrated and corrected like the rest. The resulting uplift curves are shown in Fig. 3 *a* and *b*. An age of  $31,600 \pm 300$  yr (NTU-2915), obtained on coral at 9 m on Lutaο, provides evidence for cumulative emergence, but in the absence of the requisite sea-level data, it cannot be used in the age-height plots.

Abbreviations: GPS, Global Positioning System; M, magnitude; M<sub>L</sub>, Richter magnitude.

\*E-mail: ucfcv@ucl.ac.uk.

The publication costs of this article were defrayed in part by page charge payment. This article must therefore be hereby marked "advertisement" in accordance with 18 U.S.C. §1734 solely to indicate this fact.

Article published online before print: *Proc. Natl. Acad. Sci. USA*, 10.1073/pnas.200370797. Article and publication date are at [www.pnas.org/cgi/doi/10.1073/pnas.200370797](http://www.pnas.org/cgi/doi/10.1073/pnas.200370797)

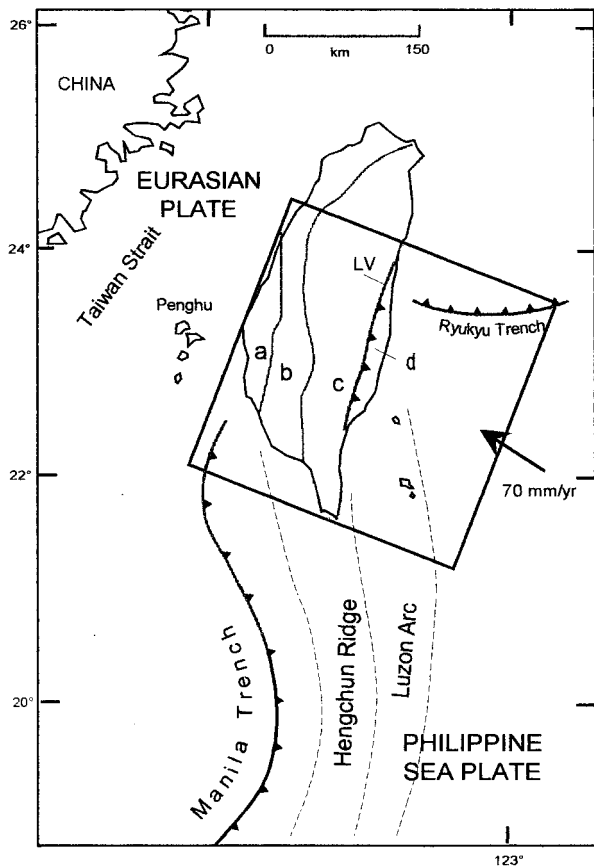


Fig. 1. Location map showing setting and major structural units of Taiwan. a, coastal plain; b, fold-and-thrust zone; c, Central Range; d, Coastal Range; LV, Longitudinal Valley. For offshore zones see text.

The graph for Lutao (Fig. 3b) is broadly equivalent to uplift at  $\approx 5$  mm/yr between 9,000 and 5,000 yr B.P. The apparent cessation of uplift after  $\approx 5,000$  yr B.P. finds support in the  $^{230}\text{Th}$ ,  $^{231}\text{Pa}$ , and  $^{14}\text{C}$  ages for the island (9), all of which are  $>5,510$  yr B.P. The data for Lanhsu (Fig. 3a) indicate continuous uplift since  $\approx 6,500$  yr B.P. but only at  $\approx 1$  mm/yr.

Holocene uplift, tilting, faulting, and folding of the Hengchun Peninsula have been reported by Liew and Lin (11) on the basis of marine terraces dated by  $^{14}\text{C}$  assay of coral fragments. Their report described buckling of a middle Holocene marine terrace that was closely linked to a thrust fault (A1) trending  $340\text{--}330^\circ$  and dipping steeply southeast with a Holocene offset of  $\approx 5$  m. Deformed river terraces suggested that upwarping near the fault amounted to as much as 15–20 m in the last 5,000–6,000 yr. Their  $^{14}\text{C}$  ages have been calibrated and corrected as for Lutao and Lanhsu and supplemented by eight additional determinations. Those listed in Table 2 and shown in Fig. 3c refer to the eastern (upthrust) block immediately east of fault A1 near Kenting. The pattern of deformation suggests that uplift is due primarily to fault-related folding.

**Geodesy.** Four medium-aperture trilateration surveys have been in operation in eastern Taiwan since 1981, of which three cross the Longitudinal Valley near Hualien, Yuli, and Taitung. The line lengths are 2–12 km, and distance assessment by electronic distance measurement (EDM) under favorable atmospheric conditions is thought to be better than  $1/10^6$  (14). Comparison between triangulation surveys conducted in 1909–1942 and in 1971 indicated left-lateral movement along the Longitudinal

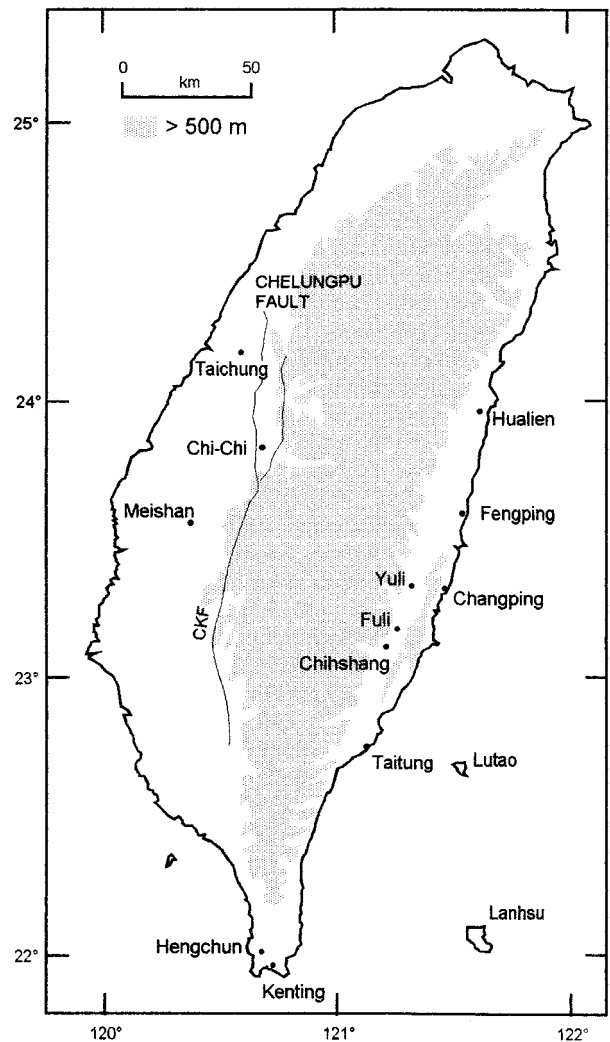


Fig. 2. Features and locations discussed in text. CKF, Chukou fault.

Valley of 30–60 mm/yr (14). The data for 1983–1988 indicate shortening across the Longitudinal Valley of 34 mm/yr ( $314^\circ$ ) at Taitung, 33 mm/yr ( $333^\circ$ ) at Yuli, and 25 mm/yr ( $0^\circ$ ) at Hualien (15). In the northern part of the valley, shear is concentrated along a single fault, whereas in the south, there is a western thrust separated by the Pinanshan Conglomerate from the strike-slip Longitudinal Valley fault to the east. Net deformation is  $\approx 28$  mm/yr at  $329^\circ$  decoupled into thrusting of 12 mm/yr at  $280^\circ$  and strike-slip of 22 mm/yr at  $353^\circ$  (16).

Close to a century of conventional geodetic data suggests that about half the plate convergence rate of 70 mm/yr is accommodated in a narrow zone centered on the Longitudinal Valley fault (15). The total rises to 52 mm/yr when the entire zone between the eastern flank of the Central Range and the islands of Lutao and Lanhsu is considered (17).

The Taiwan GPS network consists of 9 stations that are monitored continuously and 131 mobile stations that are surveyed annually. Standard errors for lengths are 5–9 mm for baselines 3–120 km long (18) or about  $1:10^7$ . Measurements between Lanhsu and Paisha (Penghu Islands), on the Eurasian plate in the Taiwan Strait, give a velocity for November 1991 through June 1995 of  $81.5 \pm 1.3$  mm/yr at  $306 \pm 1^\circ$  on a baseline measuring  $\approx 269$  km (2). The excess over the plate convergence estimate by Seno *et al.* (1) of  $\approx 70$  mm (at  $309^\circ$ ) could indicate an extensional component between Asia and the Penghu Islands (2).

**Table 1. <sup>14</sup>C ages for paleoshorelines**

| Location/elevation, m | Corrected elevation, m | <sup>14</sup> C age, yr B.P. | Calibrated age, yr B.P. | Laboratory number or source |
|-----------------------|------------------------|------------------------------|-------------------------|-----------------------------|
| <b>Lanhsu</b>         |                        |                              |                         |                             |
| 1.7                   | 1.5                    | 2,350 ± 150                  | 1,950 ± 185             | UCL-431                     |
| 2.8                   | 3                      | 1,950 ± 150                  | 1,500 ± 180             | UCL-432                     |
| 2.8                   | 2.5                    | 2,900 ± 200                  | 2,700 ± 350             | UCL-435                     |
| 3.2                   | 3                      | 2,650 ± 150                  | 2,320 ± 190             | UCL-433                     |
| 3.3                   | 3                      | 3,100 ± 150                  | 2,815 ± 210             | UCL-434                     |
| 5                     | 4                      | 4,800 ± 200                  | 5,035 ± 275             | UCL-426                     |
| 5                     | 4.5                    | 4,950 ± 200                  | 5,290 ± 310             | UCL-436                     |
| 5                     | 6                      | 6,000 ± 250                  | 6,400 ± 300             | UCL-468                     |
| 5.5                   | 6                      | 5,800 ± 250                  | 6,210 ± 290             | UCL-428                     |
| 5.5                   | 4.5                    | 4,600 ± 200                  | 4,815 ± 295             | UCL-430                     |
| 7.5                   | 7.1                    | 5,150 ± 200                  | 5,525 ± 245             | UCL-437                     |
| <b>Lutao</b>          |                        |                              |                         |                             |
| 0.75                  | 0.5                    | 5,150 ± 200                  | 5,525 ± 395             | UCL-439                     |
| 1                     | 24.5                   | 8,850 ± 70                   | 9,455 ± 165             | LT76-03                     |
| 1.3                   | 20                     | 8,500 ± 350                  | 9,055 ± 505             | UCL-438                     |
| 1.5                   | 2                      | 5,780 ± 40                   | 6,190 ± 100             | NTU-2897                    |
| 1.65                  | 0.5                    | 4,850 ± 200                  | 5,130 ± 550             | UCL-441                     |
| 1.95                  | 6                      | 6,970 ± 70                   | 7,410 ± 125             | LT76-06                     |
| 3.2                   | 2                      | 4,600 ± 200                  | 4,815 ± 295             | UCL-440                     |
| <b>Hengchun</b>       |                        |                              |                         |                             |
| 1                     | 1                      | 1,580 ± 120                  | 1,130 ± 235             | A                           |
| 1.5                   | 1.5                    | 1,710 ± 110                  | 1,260 ± 240             | A                           |
| 1.5                   | 1.5                    | 1,780 ± 115                  | 1,300 ± 245             | A                           |
| 12                    | 11                     | 4,310 ± 120                  | 4,410 ± 385             | A                           |
| 14                    | 13.5                   | 3,900 ± 125                  | 3,850 ± 360             | A                           |
| 14                    | 13.5                   | 4,040 ± 120                  | 4,060 ± 335             | A                           |
| 14                    | 13                     | 4,600 ± 400                  | 4,815 ± 930             | A                           |
| 15                    | 14.5                   | 5,000 ± 300                  | 5,310 ± 785             | A                           |
| 15                    | 14.5                   | 5,670 ± 140                  | 6,065 ± 330             | A                           |
| 15                    | 14.5                   | 5,000 ± 400                  | 5,310 ± 1,035           | A                           |
| 15                    | 48                     | 9,600 ± 1,000                | 10,290 ± 2,820          | A                           |
| 20                    | 20                     | 5,200 ± 95                   | 5,570 ± 255             | A                           |
| 20                    | 31                     | 8,410 ± 155                  | 8,965 ± 465             | A                           |
| 20                    | 42                     | 8,660 ± 155                  | 9,310 ± 395             | A                           |
| 22                    | 31                     | 7,810 ± 115                  | 8,215 ± 250             | A                           |

LT76 ages (uncalibrated) from ref. 9; A ages (uncalibrated) from ref. 11; UCL ages, this study, by first-order method (12). Heights corrected after sea-level data of W.R. Peltier (personal communication) rounded to nearest 0.5 m. Age calibration after ref. 13 is expressed as ± average error at 2  $\sigma$ . No <sup>13</sup>C correction.

Average length changes on 548 baselines over a similar period (November 1991 through June 1995) have been used to estimate station velocities relative to Paisha in the Penghu Islands. In the Coastal Range, the velocities greatly increased north of Fengping, perhaps a symptom of active reverse faulting (2, 7). They also indicate extension across the southern Central Range, which, to judge from the coastal evidence in the Hengchun Peninsula, may be a superficial effect of reverse faulting. Pronounced strain accumulation was identified within a wide zone on either side of the Chukou fault (Fig. 2; ref. 2). These findings are generally endorsed by the average principal strain rates calculated for a series of subnets in the southern Taiwan GPS network. However, to permit direct comparison with geophysical and seismic data, it is helpful to make the strain assessment on an azimuth close to 309°.

Table 2 lists linear strain measurements (i.e., length change on baseline in mm/yr per mm) for a series of baselines linking Lutao and Paisha (Penghu Islands), a total distance of 223 km. The prominence of the Longitudinal Valley and the Chukou fault zone is further emphasized. Note also the minor extension in the Coastal Range, which, like that recorded in the Central Range, could result from fault-related folding.

**Fault Slip.** Bonilla (19) reported nearly 50 Pleistocene or younger faults on Taiwan with surface breaks. In the period 1906–1951, two in the Longitudinal Valley and four in western Taiwan had coseismic displacements of 1–3 m. For example, a fault trace over 13 km long formed near Meishan in western Taiwan in 1906 during an earthquake of magnitude ( $M$ ) = 7.1 and was characterized by a displacement equivalent to 2.7 m of oblique slip. In November 1951, near Yuli, an earthquake of  $M$  = 7.3 produced a break  $\approx$ 40 km long, equivalent to 2.08 m of left-reverse oblique slip.

Aseismic fault slip also seems to achieve substantial topographic effects. Leveling indicates that, between 1983 and 1988, the eastern side of the Longitudinal Valley fault underwent uplift by fault creep at  $\approx$ 10–20 mm/yr, with the maximum of 21 mm/yr in its central segment; the horizontal component of deformation across the Longitudinal Valley, again in the central tract, also included a significant (although uncertain) component of fault creep (8). On the Chihshang fault segment, during 1990–1994, the displacement of concrete structures amounted to reverse slip at 27–37 mm/yr on a fault plane striking 018° on average and dipping 39–45° east, equivalent to shortening of 20–22 mm/yr at 313–326° (20).

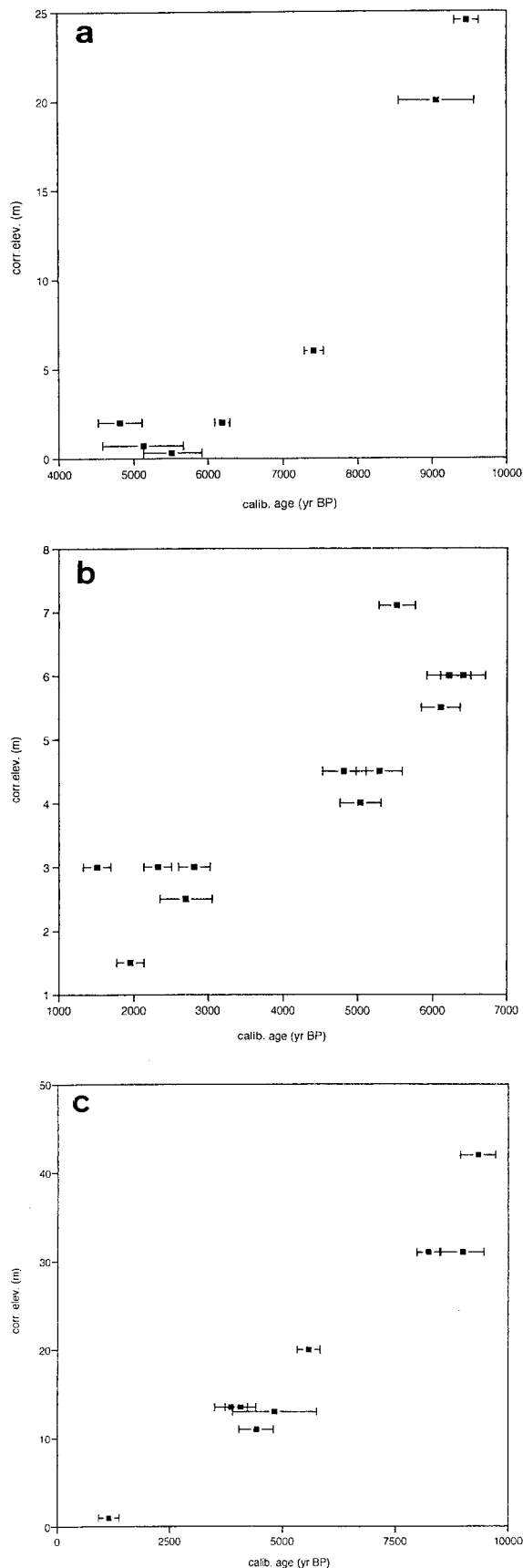


**Fig. 3.** Uplift rates based on paleoshorelines dated with calibrated (calib.)  $^{14}\text{C}$  ages corrected for sea-level change (corr. elev.; see text) for Lanhsu (a), Lutao (b), and Hengchun (c).

**Table 2.** Global Positioning System (GPS) baseline data used in present study

| Zone                 | Baseline   | Length, km | Shortening, mm/yr | $\mu\text{strain/yr}$ |
|----------------------|------------|------------|-------------------|-----------------------|
| Lutao Coast          | S063-S054  | 32.2       | 19.3              | -0.6                  |
| Coastal Range        | S054-Q207  | 5.8        | -0.6              | 0.1                   |
| Longitudinal Valley  | 0207-S045  | 9.8        | 29.6              | -3.0                  |
| Central Range        | S045-7205  | 38.9       | -8.6              | 0.2                   |
| Fold-and-thrust belt | 7205-S065  | 16.6       | 5.6               | -0.3                  |
|                      | S065-S066  | 13         | 4.2               | -0.3                  |
|                      | S066-S007* | 14.8       | 20.0              | -1.4                  |
| Coastal Plain        | S007-S004  | 24.4       | 11.6              | -0.5                  |
| Coast Paisha         | S004-S01R  | 68         | -2.4              | 0.04                  |
| Lutao Paisha         |            | 223        | 78.7              |                       |

Data from ref. 18. Error values have been omitted for clarity.  
\*Chukou fault.

The complementary basis for assessing seismic strain release is, of course, seismic moment. Pezzopane and Wesnousky (6) investigated 15 large events (with body wave magnitudes  $> 6$ ) that occurred near Taiwan in 1963–1986. Smaller events were disregarded on the grounds that they do not contribute significantly to total moment seismic release. Three of the events were associated with the Ryukyu subduction zone, and one was associated with a weakly developed, east-dipping Benioff–Wadati zone off the southeast coast of Taiwan. The remainder had depths of 13–28 km, and their focal plane solutions show either compressive or strike-slip mechanisms in a pattern indicative of distributed deformation; three of these may result from collision between the subducting Philippine Sea plate and the crust of Taiwan.

Of the remaining eight, one [1964.1.18; Richter magnitude ( $M_L$ ) = 6.5] occurred in the fold-and-thrust belt; the remainder are on the east coast or east of it. They can be accommodated by a seismogenic volume that trends  $293^\circ$  and indicates shortening by 26–54 mm/yr (6) (box in Fig. 1). The somewhat larger box required to include historical events since 1700 gives an average rate of 34–43 mm/yr. A third possibility for explaining the deficit, besides aseismic deformation and a misleading long-term average, is evidently that much of the strain is released by large, low-frequency events.

The fold-and-thrust belt has registered five earthquakes of  $M > 6.5$  in the last century, namely 1906.3.17 ( $M_L = 7.1$ ), 1935.4.21 ( $M_L = 7.1$ ), 1941.12.17 ( $M_L = 7.1$ ), 1964.1.18 ( $M_L = 6.5$ ), and 1999.9.21 ( $M_L = 7.3$ ; moment magnitude = 7.5; refs. 6, 21, and 22). The last struck near Chi-Chi (Fig. 2). The teleseismic data point to an origin on a branch of the Chukou fault, the Chelungpu fault, which has thrust Plio-Pleistocene strata over Holocene sediments a few kilometers east of the inferred deformation front (23). Surface breaks, both vertical reverse and left lateral, were reported along 105 km of the fault, which dips  $30\text{--}60^\circ$  east. Coseismic horizontal displacement determined by GPS attained a maximum of 7.1 m north-northwest: a century's worth of shortening at current rates. The main shock occurred on a thrust dipping  $20\text{--}30^\circ$  south-southeast down to a depth of  $\approx 15$  km (22). Large aftershocks indicate a second seismic zone 15 km below the main seismogenic thrust (22).

## Discussion

The three data sets used in the above review permit some items to be downgraded and others to be reinforced. Holocene deformation of the Hengchun Peninsula tallies with location within an accretionary prism immediately to the east of the



Manila trench (11, 24). Thrust fault A1, which is part of a local system of reverse faults (11), may represent one of the imbricate faults of the prism. Taking the fault dip to be 45°, the observed uplift on fault A1 could result from contraction at 5 mm/yr. Additional shortening is probably accommodated by a zone of deformation 6 km west of fault A1 (11), a major high-angle thrust 8 km east of it, and several anticlines (some of them overturned) parallel to the major thrusts (25). The observed geodetic extension emerges as a secondary, surface symptom of subsurface shortening.

Earlier work suggests that the same may apply in the Coastal Range. Motion on reverse faults is manifested here by a process of serial faulting analogous to that reported off Sumatra, where oblique convergence leads to episodes of imbricate fault reactivation separated by phases of quiescence, and activity shifts preferentially toward the subducted plate as successive imbricate reverse faults are rotated into relative inactivity (26).

Changes in the elevation of benchmarks in the Coastal Range between 1984 and 1987 and microseismic records for 1980–1983 point to activity on several parallel thrust faults (27). Although much of the displacement is by creep, coseismic movement occurs. The aftershocks of the 1986.5.20 Hualien earthquake, for example, delineated a thrust fault dipping 50–60° southeast (28). The discrepancy between Holocene shortening rates on the coast and that indicated by geodesy is readily explained by serial deformation across strike.

The uplift record of Lutao and Lanhsu is more problematic. The islands are part of the Luzon arc (Fig. 1), and their development might be viewed as purely the outcome of local volcanic activity: Lutao first erupted 0.5 million yr ago, and Lanhsu first erupted 1.4 million yr ago (29). No evidence for back-arc thrusting has been observed in the offshore part of the arc (29). But the morphology of the Luzon subduction system becomes complicated where it collides with the Chinese continental margin (30, 31). The available <sup>14</sup>C ages (Table 1) may in fact indicate progressive uplift southward, with emergence at

Lutao apparently ending ≈5,000 yr ago and affecting Lanhsu (at a slower rate) throughout the last ≈6,500 yr.

Only two structural zones emerge as subject to rapid shortening at seismic and geodetic scales, namely the Longitudinal Valley and the fold-and-thrust belt. In the former, the total geodetic signal can be disaggregated into reverse faulting and strike-slip components, in its southern portion respectively 12 mm/yr (329°) and 22 mm/yr (353°) (16), and has been ascribed to the combined effect of rapid aseismic slip and the small aperture of the geodetic network (18). On the other hand, although less than half the interplate convergence is taken up by the fold-and-thrust belt (17), its fault geometry seems propitious for seismic strain release. The Chelungpu fault has been termed an out-of-sequence thrust, because it has remained active in the hinterland of a fold-and-thrust belt (22), but, as in other convergent settings dominated by reverse faulting (26, 33), activity continues well to the rear of the deformation front until halted by progressive steepening of the faults in question. The resulting deformation gradient across strike, rather than simple strain accumulation, may explain why GPS measurements in 1993–1997 across the central Chukou fault showed that shortening increased from ≈20 mm/yr about 10 km west of the fault to ≈40 mm/yr about 20 km east of it (32).

In short, a combination of space geodesy and neotectonic analysis helps to identify structural belts above subduction zones whose geometry is suited both to the storage of strain and to its subsequent release as major earthquakes. But the location of these events within the belts cannot be specified: the instrumental record is too short for effective evaluation of models invoking seismic gaps or asperities, and the stress field is likely to be perturbed by the larger events.

I thank Jiun-Chuan Lin and Penelope Vita-Finzi for field assistance, Roger Bilham, Char-Shine Liu, and Gerald Roberts for their comments on a draft of the paper, the Royal Society and the National Science Council, Taiwan, for support, and the National Taiwan University for <sup>14</sup>C ages.

- Seno, T., Stein, S. & Gripp, A. E. (1993) *J. Geophys. Res.* **98**, 17941–17948.
- Yu, S.-B., Chen, H.-Y. & Kuo, L.-C. (1997) *Tectonophysics* **274**, 41–59.
- Suppe, J. (1987) in *The Anatomy of Mountain Ranges*, eds. Schaer, J.-P. & Rodgers, J. (Princeton Univ. Press, Princeton, NJ), pp. 277–293.
- Ho, C. S. (1982) *Tectonic Evolution of Taiwan* (Minist. Econ. Aff., Taipei, Taiwan).
- Lundberg, N., Reed, D. L., Liu, C. S. & Lieske, J., Jr. (1992) *Acta Geol. Taiwanica* **30**, 131–140.
- Pezzopane, S. K. & Wesnousky, S. G. (1989) *J. Geophys. Res.* **94**, 7250–7264.
- Vita-Finzi, C. & Lin, J.-C. (1998) *Geology* **26**, 279–281.
- Yu, S.-B. & Liu, C.-C. (1989) *Proc. Geol. Soc. China* **32**, 209–231.
- Wang, C.-H., Burnett, W. C., Yu, E.-F. & Tai, W.-C. (1988) *Radioisotopic Studies of Fossil Corals from Lanyu and Lutao Islands* (Inst. Earth Sci., Academia Sinica, Taipei, Taiwan).
- Peng, T.-H., Li, Y.-H. & Wu, F. T. (1977) *Mem. Geol. Soc. China* **2**, 57–69.
- Liew, P.-M. & Lin, C.-F. (1987) *Mem. Geol. Soc. China* **9**, 241–259.
- Vita-Finzi, C. (1983) *Earth Planet. Sci. Lett.* **65**, 389–393.
- Stuiver, M. & Reimer, P. J. (1993) *Radiocarbon* **19**, 355–363.
- Yu, S.-B. & Lee, C. (1986) *Tectonophysics* **125**, 73–85.
- Yu, S.-B., Jackson, D. D., Yu, G.-K. & Liu, C.-C. (1990) *Tectonophysics* **183**, 97–109.
- Lee, J.-C., Angelier, J., Chu, H.-T., Yu, S.-B. & Hu, J.-C. (1998) *Tectonics* **17**, 859–871.
- Lundberg, N., Reed, D. L., Liu, C. S. & Lieske, J., Jr. (1997) *Tectonophysics* **274**, 5–23.
- Yu, S.-B. & Chen, H.-Y. (1994) *Terr. Atmos. Oceanic Sci.* **5**, 477–498.
- Bonilla, M. G. (1977) *Mem. Geol. Soc. China* **2**, 43–55.
- Angelier, J., Chu, H.-T. & Lee, J.-C. (1997) *Tectonophysics* **274**, 117–143.
- Ma, K.-F., Lee, C.-T. & Tsai, Y.-B. (1999) *EOS Trans. Am. Geophys. Union* **80**, 605, 611.
- Kao, H. & Chen, W.-P. (2000) *Science* **288**, 2346–2349.
- Huang, C.-Y., Huang, C.-S., Chen, Y.-G., Lee, J.-F., Lee, Y.-H., Chen, M.-M. & Wu, W.-Y. (1999) *Field Trip Guide to Seismic Geology, Central Taiwan* (Nat. Sci. Mus., Taichung, Taiwan).
- Liu, C.-S., Huang, I. L. & Teng, L. S. (1997) *Mar. Geol.* **137**, 305–319.
- Geological Map of Taiwan (1991) *Sheet 69, 70, 72, 1/100,000* (Central Geological Survey, Taipei, Taiwan).
- Vita-Finzi, C. (1996) *J. Coastal Res. Spec. Issue* **17**, 279–281.
- Liu, C.-C. & Yu, S. B. (1990) *Tectonophysics* **183**, 111–119.
- Shin, T.-C., Xhang, Z.-S. & Yu, G.-K. (1989) *Proc. Geol. Soc. China* **32**, 233–253.
- Lundberg, N., Reed, D. L., Liu, C. S. & Lieske, J., Jr. (1997) *Tectonophysics* **274**, 5–23.
- Liu, C.-S., Liu, S.-Y., Lallemand, S. E., Lundberg, N. & Reed, D. L. (1998) *Terr. Atmos. Oceanic Sci.* **9**, 705–738.
- Kao, H., Huang, G.-C. & Liu, C.-S. (2000) *J. Geophys. Res.* **105**, 3059–3079.
- Yu, S.-B. & Chen, H.-Y. (1998) *Terr. Atmos. Oceanic Sci.* **9**, 31–50.
- Mann, C. D. & Vita-Finzi, C. (1988) *Geol. Soc. London Spec. Pub.* **37**, 51–59.